Water Year 2021 Compound Precipitation and Temperature Extremes in California and Nevada

Andrew Hoell, Xiao-Wei Quan, Martin Hoerling, Henry F. Diaz, Rong Fu, Cenlin He, Joel R. Lisonbee, Justin S. Mankin, Richard Seager, Amanda Sheffield, Isla R. Simpson, and Eugene R. Wahl

AFFILIATIONS: Hoell and Hoerling—NOAA/Physical Sciences Laboratory, Boulder, Colorado; **Quan**—NOAA/Physical Sciences Laboratory, and Cooperative Institute for Research in Environmental Sciences, University of Colorado Boulder, Boulder, Colorado; **Diaz**—Department of Geography and Environment, University of Hawai'i at Mānoa, Honolulu, Hawaii; **Fu**—Department of Atmospheric and Oceanic Sciences, University of California, Los Angeles, Los Angeles, California; **He**—Research Applications Laboratory, National Center for Atmospheric Research, Boulder, Colorado; **Lisonbee and Sheffield**—Cooperative Institute for Research in Environmental Sciences, University of Colorado Boulder, and NOAA/National Integrated Drought Information System, Boulder, Colorado; **Mankin**—Dartmouth College, Hanover, New Hampshire; **Seager**—Lamont-Doherty Earth Observatory, Columbia University, Palisades, New York; **Simpson**—Climate and Global Dynamics Laboratory, National Center for Atmospheric Research, Boulder, Colorado; **Wahl***—NOAA/National Centers for Environmental Information, Boulder, Colorado
* Retired

DOI: https://doi.org/10.1175/BAMS-D-22-0112.1

CORRESPONDING AUTHOR: Andrew Hoell, andrew.hoell@noaa.gov

Supplemental material: https://doi.org/10.1175/BAMS-D-22-0112.2

In final form 12 August 2022

KEYWORDS: Drought; Heat Wave; Anthropogenic effects/forcing; La Nina

Anthropogenically forced-warming and La Niña forced-precipitation deficits caused at least a sixfold risk increase for compound extreme low precipitation and high temperature in California–Nevada from October 2020 to September 2021.

The most intense 22-yr drought in the western United States since 800 CE (Williams et al. 2022) was extended by compound dry and hot extremes in Water Year 2021 (October 2020–September 2021). Compared to an instrumental record that dates to 1895, low precipitation (Fig. 1a) and high temperatures (Fig. 1b) were widespread across the western United States. The intense and prevalent drought has caused water delivery shortages (U.S. Bureau of Reclamation 2021), damaged ecosystems (Wlostowski et al. 2022), and contributed to extreme wildfires (e.g., Fu et al. 2021; Gutierrez et al. 2021; Abolafia-Rosenzweig et al. 2022).

California and Nevada (CA–NV) were once again at the epicenter of drought and heat in Water Year 2021 (California Department of Water Resources 2021). This was the first time since 1895 that precipitation fell below −1.5 standardized departures and temperatures exceeded 1.5 standardized departures concurrently for the two-state average (Fig. 1c). Precipitation and temperatures were individually extreme as well, as the former was the second lowest since 1895 and the latter was the second highest.

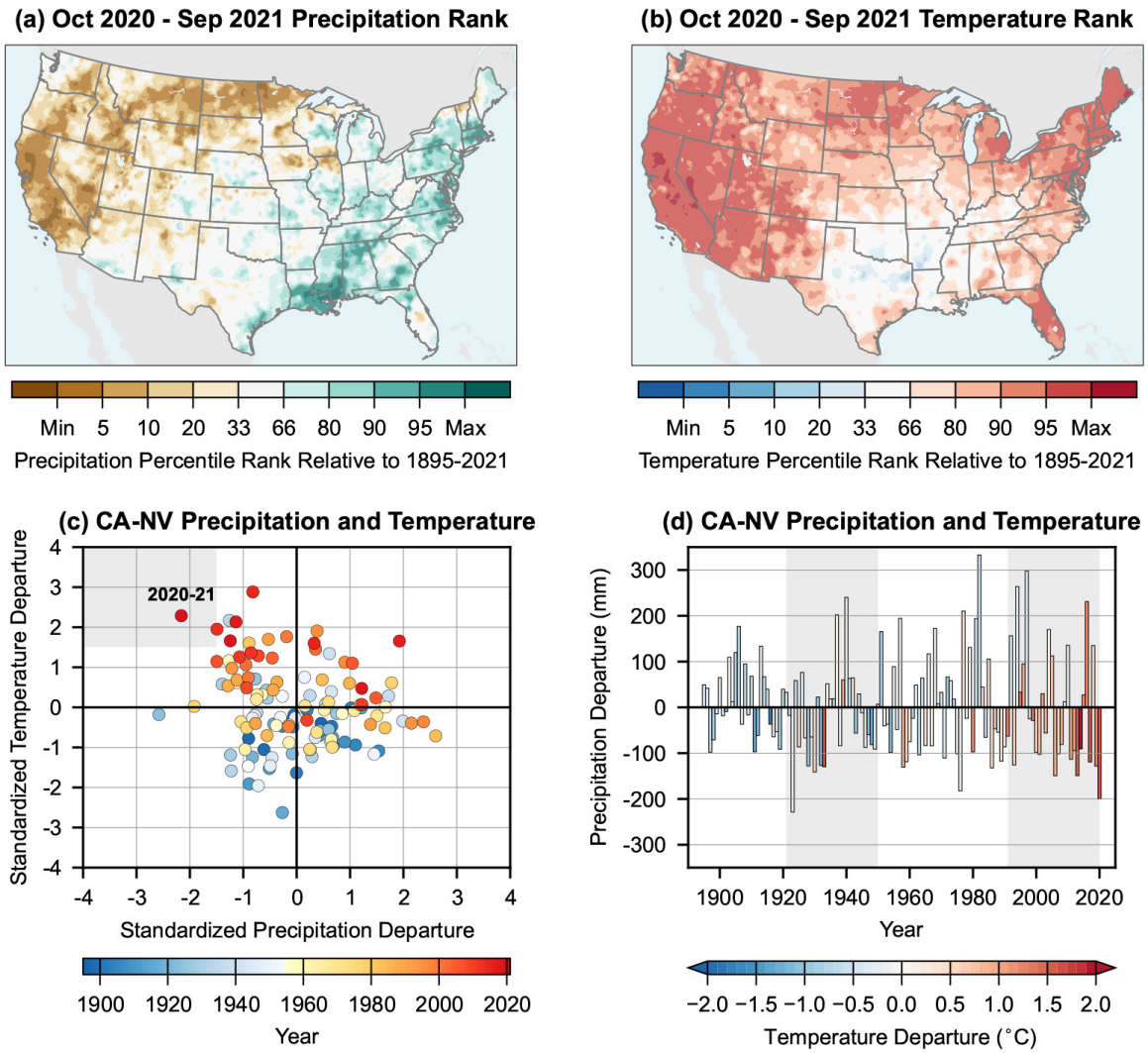

Fig. 1. Estimates of observed percentile ranks for October 2020–September 2021 relative to 1895–2021 in terms of (a) precipitation and (b) temperature. For CA–NV during October–September relative to 1895–2021, (c) scatter relationship between observed standardized temperature and standardized precipitation and (d) time series of observed precipitation (bars; mm) and temperature (shading within bars; °C) departure from average. The gray shading in (c) indicates the location where precipitation is lower and temperature is higher than 1.5 standard deviations from the average and the gray shading in (d) indicates past (1921–50) and recent (1991–2020) climates.

We examine whether the co-occurrence of anthropogenic climate change and La Niña,[1] two principal climate drivers during Water Year 2021, altered the risk of unprecedented compound dry and hot extremes in CA–NV during Water Year 2021. Our assessment investigates the factors related to compound extremes that lead to heightened societal impacts compared to individual extreme events (e.g., AghaKouchak et al. 2020; Zscheischler et al. 2020; W. Zhang et al. 2021).

[1] https://origin.cpc.ncep.noaa.gov/products/analysis_monitoring/ensostuff/ONI_v5.php

Data and methods

Data. Estimates of observed precipitation and temperature since 1895 are from nClimGrid/CLIMGRID (Vose et al. 2014) and estimates of observed sea surface temperatures (SST) over the same period are from the Extended Reconstructed SST version 5 (Huang et al. 2017). Simulated

Table 1. Model ensembles used.

Model ensemble	Reference	Ensemble size	Historical period	Future period and forcing
Coupled Model Intercomparison Project phase 6 (CMIP6)	Eyring et al. (2016)	38	Before 2015	After 2015 and SSP5–8.5 (Eyring et al. 2016)
Seamless System for Prediction and Earth System Research (SPEAR)	Delworth et al. (2020)	30	Before 2015	After 2015 and SSP5–8.5 (Eyring et al. 2016)
Community Earth System Model version 1 (CESM1)	Kay et al. (2015)	40	Before 2005	After 2005 and RCP8.5 (Taylor et al. 2012)
Community Earth System Model version 2 (CESM2)	Danabasoglu et al. (2020)	100	Before 2015	After 2015 and SSP3–7.0 (Eyring et al. 2016)

quantities are from four fully coupled transient climate model ensembles (Table 1) in which time-evolving natural and anthropogenic forcings are prescribed, such as greenhouse gasses and aerosols (J. Zhang et al. 2021). The CMIP6 ensemble used here consists of a single realization from 38 different models (Table ES1 in the supplemental material) and the SPEAR, CESM1, and CESM2 ensembles consist of many realizations from their namesake models, which differ in their representation of internal variability due to perturbations introduced at initialization. The suitability of the models regarding the seasonality of precipitation and temperature and their relationship with ENSO in CA–NV are discussed in the supplemental text and Fig. ES1.

Methods. Three indices are used to describe climate conditions. Precipitation and temperature indices for CA–NV during the water year in observed estimates and in each model realization are computed from an average of all grid points in the two states. Precipitation and temperature indices are standardized after averaging over the two states. The Niño-3.4 index during October–May is used to quantify the state of El Niño–Southern Oscillation, given this is the CA–NV wet season and time of maximal ENSO amplitude (e.g., Chen and Jin 2020). The Niño-3.4 index (Bamston et al. 1997) is computed in observed analyses and in model simulations from an average of all SST grid points within 5°S–5°N, 120°–170°W. La Niña is defined as a −1 standardized departure in the Niño-3.4 index, as was observed in 2020–21.

Different climate conditions are compared in the model simulations to estimate the effects of anthropogenic influences and La Niña on the risk of compound hot (temperature exceeding 1.5 standardized departures) and dry (precipitation falling below −1.5 standardized departures) extremes in CA–NV during the water year. To deconvolve their respective influences on compound hot and dry extremes, temperature and precipitation are examined during La Niña conditions in recent and past climates in model ensembles. The effect of La Niña is diagnosed by comparing simulated conditions during La Niña years to the remaining "non–La Niña" years. Anthropogenic influences are diagnosed by comparing quantities from the past (1921–50) climate to those from the recent (1991–2020) climate. The 1921–50 period is used as the past or counterfactual climate because it is the period in which western U.S. water policy was written, water management practices were developed, and hydrologic infrastructure was built. In contrast to a preindustrial baseline, as is often used, the 1921–50 period represents the climate normal to which people and policy are well adapted. Precipitation and temperature are standardized relative to 1921–2020 and the Niño-3.4 index is standardized relative to each climate epoch to accentuate interannual variability, consistent with the NOAA Climate Prediction Center's definition of El Niño–Southern Oscillation events.[2] The relative risk ratio (e.g., Otto et al. 2018) is used to quantify the effects of anthropogenic and La Niña influences on compound hot and dry extremes during the water year. Relative risk confidence intervals are calculated via bootstrapping (see supplemental text).

[2] https://origin.cpc.ncep.noaa.gov/products/analysis_monitoring/ensostuff/ONI_change.shtml

Results

Observed analyses. CA–NV climate exhibits strong interannual precipitation variability (Fig. 1d) having a 25% coefficient of variation, although with a lag-1 autocorrelation of only −0.01 for the entire period of record, which is indicative of little interannual memory (e.g., Dettinger et al. 1998; Wang et al. 2017; Wahl et al. 2020). The interannual variability is shaped in part by ENSO (e.g., Schonher and Nicholson 1989), given the correlation between CA–NV precipitation and the Niño-3.4 index of 0.33 ($p < 0.05$) in the recent climate (Fig. ES1c), which confirms that below-average CA–NV water year precipitation is related to La Niña. Despite the pronounced low precipitation since the turn of the twenty-first century related to decadal variations in Pacific Ocean SSTs (Lehner et al. 2018), there is no significant precipitation trend from 1895 to 2021. Regarding temperature, the most striking feature of its time series is the pronounced warming trend throughout the instrumental record, which has been especially strong since the mid-1990s (Figs. 1c,d). There is only modest covariability of CA–NV temperature and precipitation, with a weak October–September correlation of −0.18 (Fig. 1c).

Model simulations. Given the brevity of—and the large interannual variability in—the observed record, change detection is difficult, especially for precipitation (Fig. 1). We therefore examine the effects of anthropogenic climate change and La Niña on compound hot and dry extremes using ensembles of climate models. Comparing past and recent climates, with the latter conditioned on La Niña to reflect the internal climate state of 2021, the risk of compound dry and hot extremes significantly increases by at least 6 times in the recent period in the model ensembles (Table 2, top row). Some variation in the risk of these compound extremes is noted between the model ensembles, with the SPEAR ensemble indicating a sixfold increase and the CESM1 ensemble indicating a nearly twelvefold increase.

Table 2. Relative risk ratio and its 95% confidence interval (in brackets) of temperature exceeding 1.5 standardized departures and precipitation falling below –1.5 standardized departures simultaneously in CA–NV during October–September.

	CMIP6	SPEAR	CESM1	CESM2
Past non–La Niña to Recent La Niña	7.9 [3.8, 18.6]	6.1 [2.6, 14.5]	11.7 [6.6, 23.4]	7.4 [4.2, 13.7]
Past La Niña to Recent La Niña	4.1 [1.7, 14.9]	5.1 [1.7, 22.1]	4.3 [2.3, 10.3]	5.4 [2.8, 13.8]
Past non–La Niña to Recent non-La Niña	4.0 [2.0, 9.3]	4.9 [2.9, 10.7]	4.3 [2.4, 9.8]	5.9 [3.7, 10.7]
Recent non–La Niña to Recent La Niña	1.1 [0.0, 4.0]	1.6 [0.3, 4.4]	4.9 [0.9, 21.8]	3.2 [1.1, 7.9]

The increase in the risk of compound dry and hot extremes is the result of statistically significant shifts to both lower precipitation and higher temperatures, a response evident in all four models (Figs. 2a–d). Different forcings contribute to different elements of the compound risk, however. La Niña forces the lower precipitation via interannual ENSO teleconnections that increase dry extreme risks over the western United States (Figs. ES2a–d). Anthropogenic forcing increases regional temperatures, with the models differing somewhat in their spatial pattern of temperature risk (Figs. ES2e–h).

The middle two rows of Table 2 and Fig. 2 present the separate effects of anthropogenic and interannual La Niña forcings on the risk of compound hot and dry extremes during the water year over CA–NV. We note similarities in the risk ratios and their confidence intervals among the models and two cases considered (cf. Past La Niña to Recent La Niña and Past non–La Niña to Recent non–La Niña) and that some models arrived at these risk ratios in different ways due to slight differences in their sensitivities to the drivers they are conditioned on. Comparing past to recent climates conditioned on La Niña, a statistically significant increase in the risk

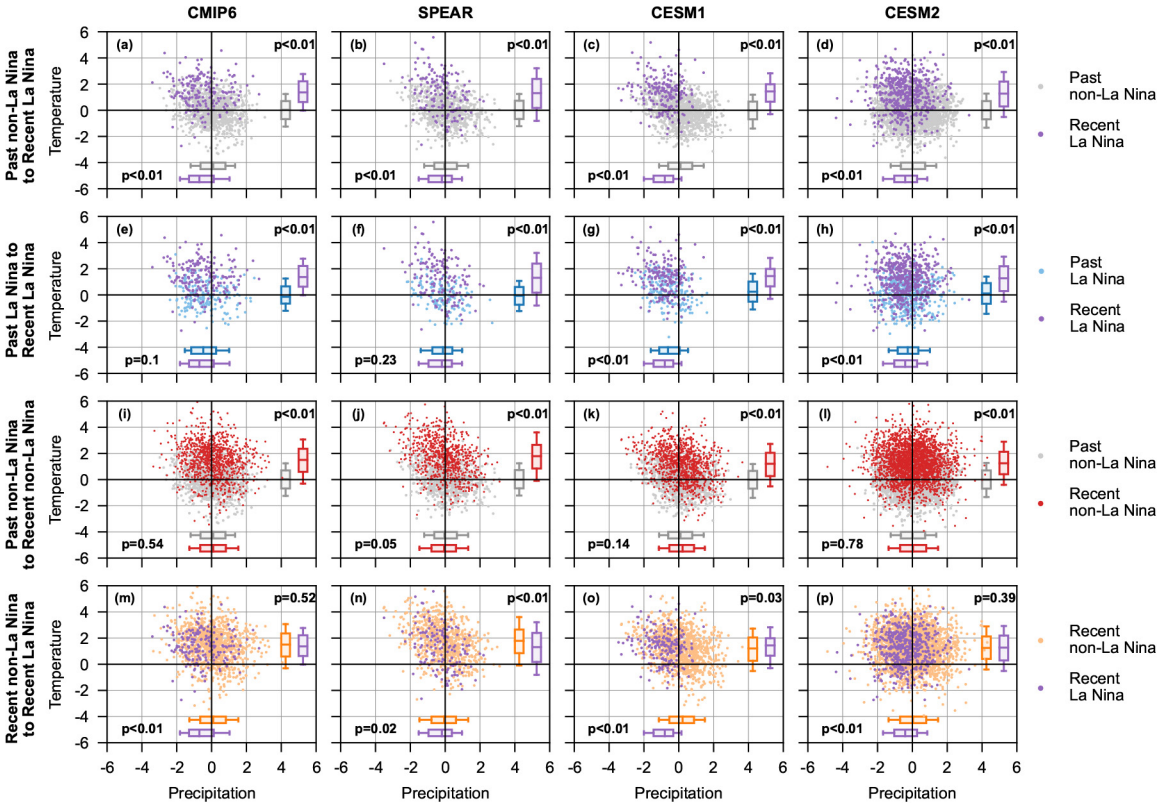

Fig. 2. Scatterplots of the relationship between standardized temperature and standardized precipitation in the four model ensembles for (a)–(d) past climate non–La Niña (gray) and recent climate La Niña (purple), (e)–(h) past climate La Niña (blue) and recent climate La Niña (purple), (i)–(l) past climate non–La Niña (gray) and recent climate non–La Niña (red), and (m)–(p) recent climate non–La Niña (orange) and recent climate La Niña (purple). Colored boxplots indicate the temperature and precipitation distributions, where boxes indicate the interquartile range and the whiskers indicate the interdecile range. The p values are from a two-sided t test of the precipitation and temperature distributions of the two samples.

of compound hot and dry extremes during the water year of at least 4 times is noted in all model ensembles (Table 2, second row from top). The increase in the compound risk is principally caused by high temperatures, as models indicate large and statistically significant shifts to higher temperatures from past to recent climates while only two models, both from the CESM family, indicate small though significant shifts to lower precipitation (Figs. 2e–h). A statistically significant increase in the risk of hot extremes is found over almost the entire contiguous United States, with the largest increases west of the Rockies in three of the four model ensembles (Figs. ES2m–p). Spatial patterns of the risk in low water year precipitation is suggested by attendant patterns of change in the four model ensembles, and particularly the CESM family (Figs. ES2i–l). Comparing past to recent climates without La Niña also indicates a statistically significant increase in the risk of compound hot and dry extremes during the water year of at least 4 times in all model ensembles (Table 2, second row from bottom) that is also principally caused by temperatures, as indicated by statistically significant shifts to higher temperatures and no significant change in precipitation (Figs. 2i–l; Figs. ES2q–x).

To isolate the effects of La Niña alone, we compare conditions during the recent climate for La Niña years versus non-La Niña years. We find no statistically significant evidence for an increase in the risk of both hot and dry extremes during the water year related to La Niña in the recent climate (Table 2, bottom row). However, La Niña itself leads to statistically significant shifts in the precipitation distribution to drier conditions in CA–NV (Figs. 2m–p),

which is associated with the relationship between ENSO and precipitation over the western and southern tier of the United States (Figs. ES2y–bb). La Niña alone does not significantly shift mean temperatures during the water year in three of the four model ensembles (Figs. 2m–p). The inverse correlation between surface air temperature and precipitation, caused by shifts in the surface energy balance as soil moisture and evapotranspiration change, and which is often invoked to explain concurrent heat and drought, is largely restricted to the warm season and the interior continent and not operative in the cool season in the CA–NV region (not shown).

Conclusions and discussion

Coupled climate model ensembles indicate that anthropogenic climate change and La Niña, presumed to be the primary climate drivers in 2021, together led to a greater than sixfold increase in the risk of compound hot and dry extremes (each greater than 1.5 standard departures) from October 2020–September 2021 in CA–NV. We found that anthropogenic effects principally caused an increase in extreme temperature risks while La Niña effects principally increased extreme low precipitation risks, though it is important to note that details diverge between climate models regarding their individual sensitivities to the aforementioned drivers. Moreover, the change in external forcing alone leads to statistically significant increases in the risk of compound temperature and precipitation extremes because of the exceptional shift to higher temperatures while La Niña alone is insufficient to do so because it is only related to significant shift to lower precipitation.

Several factors have not been addressed that could also be relevant to changing risks of compound hot and dry extremes in CA–NV. First, we have not explicitly addressed how the tropical Pacific Ocean and ENSO or its teleconnections may have changed due to anthropogenic forcing. For instance, is the observed trend toward a more La Niña–like zonal SST gradient a response to anthropogenic forcing (e.g., Hoell and Funk 2013; Coats and Karnauskas 2017)? If so, it is not simulated by CMIP class models (e.g., Seager et al. 2019, 2022) and would likely affect CA–NV precipitation (e.g., Seager and Vecchi 2010; Yoon et al. 2015; Swain et al. 2018)? Second, we have not explicitly controlled for forced changes in land–atmosphere feedbacks, which can amplify warming and drying effects. There is some evidence that temperature and precipitation correlations may have strengthened in recent decades compared to the early twentieth century. But the issue of whether anthropogenic influences change the land surface coupling, which could make droughts in CA–NV hotter, is an area of active research (Chiang et al. 2018; Cheng et al. 2019).

Acknowledgments. The authors gratefully acknowledge helpful comments from Mike Alexander on an earlier version of the manuscript and two anonymous reviewers, and support from the NOAA Climate Program Office Modeling, Analysis, Predictions, and Projections Program, the National Integrated Drought Information System, and the NOAA Physical Sciences Laboratory.

References

Abolafia-Rosenzweig, R., C. He, and F. Chen, 2022: Winter and spring climate explains a large portion of interannual variability and trend in western US summer fire burned area. *Environ. Res. Lett.*, **17**, 054030, https://doi.org/10.1088/1748-9326/ac6886.

AghaKouchak, A., and Coauthors, 2020: Climate extremes and compound hazards in a warming world. *Annu. Rev. Earth Planet. Sci.*, **48**, 519–548, https://doi.org/10.1146/annurev-earth-071719-055228.

Bamston, A. G., M. Chelliah, and S. B. Goldenberg, 1997: Documentation of a highly ENSO-related SST region in the equatorial Pacific: Research note. *Atmos.–Ocean*, **35**, 367–383, https://doi.org/10.1080/07055900.1997.9649597.

California Department of Water Resources, 2021: Water year 2021: An extreme year. 12 pp., https://water.ca.gov/-/media/DWR-Website/Web-Pages/Water-Basics/Drought/Files/Publications-And-Reports/091521-Water-Year-2021-broch_v2.pdf.

Chen, H.-C., and F.-F. Jin, 2020: Fundamental behavior of ENSO phase locking. *J. Climate*, **33**, 1953–1968, https://doi.org/10.1175/JCLI-D-19-0264.1.

Cheng, L., M. Hoerling, Z. Liu, and J. Eischeid, 2019: Physical understanding of human-induced changes in U.S. hot droughts using equilibrium climate simulations. *J. Climate*, **32**, 4431–4443, https://doi.org/10.1175/JCLI-D-18-0611.1.

Chiang, F., O. Mazdiyasni, and A. AghaKouchak, 2018: Amplified warming of droughts in southern United States in observations and model simulations. *Sci. Adv.*, **4**, eaat238, https://doi.org/10.1126/sciadv.aat2380.

Coats, S., and K. B. Karnauskas, 2017: Are simulated and observed twentieth century tropical Pacific sea surface temperature trends significant relative to internal variability? *Geophys. Res. Lett.*, **44**, 9928–9937, https://doi.org/10.1002/2017GL074622.

Danabasoglu, G., and Coauthors, 2020: The Community Earth System Model version 2 (CESM2). *J. Adv. Model. Earth Syst.*, **12**, e2019MS001916, https://doi.org/10.1029/2019MS001916.

Delworth, T. L., and Coauthors, 2020: SPEAR: The next generation GFDL modeling system for seasonal to multidecadal prediction and projection. *J. Adv. Model. Earth Syst.*, **12**, e2019MS001895, https://doi.org/10.1029/2019MS001895.

Dettinger, M. D., D. R. Cayan, H. F. Diaz, and D. M. Meko, 1998: North–South precipitation patterns in western North America on interannual-to-decadal timescales. *J. Climate*, **11**, 3095–3111, https://doi.org/10.1175/1520-0442(1998)011<3095:NSPPIW>2.0.CO;2.

Eyring, V., S. Bony, G. A. Meehl, C. A. Senior, B. Stevens, R. J. Stouffer, and K. E. Taylor, 2016: Overview of the Coupled Model Intercomparison Project phase 6 (CMIP6) experimental design and organization. *Geosci. Model Dev.*, **9**, 1937–1958, https://doi.org/10.5194/gmd-9-1937-2016.

Fu, R., A. Hoell, J. Mankin, A. Sheffield, and I. R. Simpson, 2021: Tackling challenges of a drier, hotter, more fire-prone future. *Eos*, **102**, https://doi.org/10.1029/2021EO156650.

Gutierrez, A. A., S. Hantson, B. Langenbrunner, B. Chen, Y. Jin, L. Goulden Michael, and T. Randerson James, 2021: Wildfire response to changing daily temperature extremes in California's Sierra Nevada. *Sci. Adv.*, **7**, eabe6417, https://doi.org/10.1126/sciadv.abe6417.

Hoell, A., and C. Funk, 2013: The ENSO-related west Pacific sea surface temperature gradient. *J. Climate*, **26**, 9545–9562, https://doi.org/10.1175/JCLI-D-12-00344.1.

Huang, B., and Coauthors, 2017: Extended Reconstructed Sea Surface Temperature, version 5 (ERSSTv5): Upgrades, validations, and intercomparisons. *J. Climate*, **30**, 8179–8205, https://doi.org/10.1175/JCLI-D-16-0836.1.

Kay, J. E., and Coauthors, 2015: The Community Earth System Model (CESM) large ensemble project: A community resource for studying climate change in the presence of internal climate variability. *Bull. Amer. Meteor. Soc.*, **96**, 1333–1349, https://doi.org/10.1175/BAMS-D-13-00255.1.

Lehner, F., C. Deser, I. R. Simpson, and L. Terray, 2018: Attributing the U.S. Southwest's recent shift into drier conditions. *Geophys. Res. Lett.*, **45**, 6251–6261, https://doi.org/10.1029/2018GL078312.

Otto, F. E. L., S. Philip, S. Kew, S. Li, A. King, and H. Cullen, 2018: Attributing high-impact extreme events across timescales—A case study of four different types of events. *Climatic Change*, **149**, 399–412, https://doi.org/10.1007/s10584-018-2258-3.

Schonher, T., and S. E. Nicholson, 1989: The relationship between California rainfall and ENSO events. *J. Climate*, **2**, 1258–1269, https://doi.org/10.1175/1520-0442(1989)002<1258:TRBCRA>2.0.CO;2.

Seager, R., and G. A. Vecchi, 2010: Greenhouse warming and the 21st century hydroclimate of southwestern North America. *Proc. Natl. Acad. Sci*. USA, **107**, 21 277–21 282, https://doi.org/10.1073/pnas.0910856107.

Seager, R., M. Cane, N. Henderson, D.-E. Lee, R. Abernathey, and H. Zhang, 2019: Strengthening tropical Pacific zonal sea surface temperature gradient consistent with rising greenhouse gases. *Nat. Climate Change*, **9**, 517–522, https://doi.org/10.1038/s41558-019-0505-x.

Seager, R., N. Henderson, and M. Cane, 2022: Persistent discrepancies between observed and modeled trends in the tropical Pacific Ocean. *J. Climate*, **35**, 4571–4584, https://doi.org/10.1175/JCLI-D-21-0648.1.

Swain, D. L., B. Langenbrunner, J. D. Neelin, and A. Hall, 2018: Increasing precipitation volatility in twenty-first-century California. *Nat. Climate Change*, **8**, 427–433, https://doi.org/10.1038/s41558-018-0140-y.

Taylor, K. E., R. J. Stouffer, and G. A. Meehl, 2012: An overview of CMIP5 and the experiment design. *Bull. Amer. Meteor. Soc.*, **93**, 485–498, https://doi.org/10.1175/BAMS-D-11-00094.1.

U.S. Bureau of Reclamation, 2021: Annual operating plan for Colorado River reservoirs 2022. 35 pp., https://www.usbr.gov/lc/region/g4000/aop/AOP22.pdf.

Vose, R. S., and Coauthors, 2014: Improved historical temperature and precipitation time series for U.S. climate divisions. *J. Appl. Meteor. Climatol.*, **53**, 1232–1251, https://doi.org/10.1175/JAMC-D-13-0248.1.

Wahl, E. R., A. Hoell, E. Zorita, E. Gille, and H. F. Diaz, 2020: A 450-year perspective on California precipitation "flips." *J. Climate*, **33**, 10221–10237, https://doi.org/10.1175/JCLI-D-19-0828.1.

Wang, S. Y. S., J.-H. Yoon, E. Becker, and R. Gillies, 2017: California from drought to deluge. *Nat. Climate Change*, **7**, 465–468, https://doi.org/10.1038/nclimate3330.

Williams, A. P., B. I. Cook, and J. E. Smerdon, 2022: Rapid intensification of the emerging southwestern North American megadrought in 2020–2021. *Nat. Climate Change*, **12**, 232–234, https://doi.org/10.1038/s41558-022-01290-z.

Wlostowski, A. N., K. S. Jennings, R. E. Bash, J. Burkhardt, C. W. Wobus, and G. Aggett, 2022: Dry landscapes and parched economies: A review of how drought impacts nonagricultural socioeconomic sectors in the US Intermountain West. *Wiley Interdiscip. Rev.: Water*, **9**, e1571, https://doi.org/10.1002/wat2.1571.

Yoon, J.-H., S. Y. S. Wang, R. R. Gillies, B. Kravitz, L. Hipps, and P. J. Rasch, 2015: Increasing water cycle extremes in California and in relation to ENSO cycle under global warming. *Nat. Commun.*, **6**, 8657, https://doi.org/10.1038/ncomms9657.

Zhang, J., and Coauthors, 2021: The role of anthropogenic aerosols in the anomalous cooling from 1960 to 1990 in the CMIP6 Earth system models. *Atmos. Chem. Phys.*, **21**, 18609–18627, https://doi.org/10.5194/acp-21-18609-2021.

Zhang, W., M. Luo, S. Gao, W. Chen, V. Hari, and A. Khouakhi, 2021: Compound hydrometeorological extremes: Drivers, mechanisms and methods. *Front. Earth Sci.*, **9**, 673495, https://doi.org/10.3389/feart.2021.673495.

Zscheischler, J., and Coauthors, 2020: A typology of compound weather and climate events. *Nat. Rev. Earth Environ.*, **1**, 333–347, https://doi.org/10.1038/s43017-020-0060-z.